

Spectroscopic analysis of the SB3 system 74 Aqr^{★†}

G. Catanzaro^{‡§} and F. Leone

INAF – Catania Astrophysical Observatory, Via S. Sofia 78, I–95123, Catania, Italy

Accepted 2006 September 5. Received 2006 September 4; in original form 2006 June 21

ABSTRACT

In this paper, we present the first quantitative abundance analysis of the SB3 system whose primary is the well-known mercury–manganese (HgMn) star 74 Aqr (= HD 216494). From the fit of the H β profile, obtained at the orbital phase of maximum separation between A and B components, we determined the effective temperatures and surface gravities of each component: $T_{\text{eff}}^{\text{A}} = 12\,000$ K, $\log g^{\text{A}} = 3.70$, $T_{\text{eff}}^{\text{B}} = 11\,500$ K, $\log g^{\text{B}} = 3.90$ and $T_{\text{eff}}^{\text{C}} = 11\,500$ K, $\log g^{\text{C}} = 4.10$. These values are validated by the coincidence of abundances derived from different ionization states of iron.

We find that this system is heterogeneous from the point of view of the chemical composition: HD 216494 A shows the typical spectral features, with the exception of strontium underabundance, of HgMn stars. Apart from a mild helium underabundance and overabundance of two rare earths (praseodymium and neodymium), HD 216494 B does not show any other anomaly. The fast rotating C component, in spite of the difficulties found in the identification of its spectral lines, seems to be the only normal star of the system.

Key words: stars: abundances – stars: chemically peculiar – stars: individual: 74 Aqr.

1 INTRODUCTION

Mercury–manganese stars (hereafter HgMn stars) constitute a well-defined subgroup of chemically peculiar stars of the main sequence in the temperature range 10 000–14 000 K. The most important features characterizing their peculiarities are extreme overabundances of Hg and Mn, respectively, up to 6 and 3 dex, compared to the solar case. Their chemical pattern includes also enhancement of elements such as gallium, phosphorus and strontium together with depletion of elements like nitrogen, aluminium and zinc. HgMn stars are thought to have a very stable atmosphere since they are among the most slowly rotating stars of the upper main sequence and they present very low values of microturbulent velocity. This stability plays an important role in the theory of the radiatively driven diffusion and gravitational settling developed by Michaud (1970) to explain the chemical anomalies observed in their atmospheres.

The importance of HgMn stars up to now described is particularly important when they belong to a binary or even multiple system. As many of these systems have components sufficiently far apart to

have evolved independently from the common protostellar cloud, they should be studied to understand how the peculiarities originate in stellar atmospheres.

2 THE STAR

The peculiar nature of HD 216494 (= HR 8704 = 74 Aqr) as manganese star was discovered in a survey of late B-type stars by Wolff & Wolff (1974). Assuming a SB2 system, orbital parameters have been first determined by Wolff (1974), who also confirmed the enhanced mercury abundance in the primary. The orbit solution has been improved recently by Catanzaro & Leto (2004) who determined a period of $3.429\,619 \pm 0.000\,004$ d and a mass ratio $M_{\text{A}}/M_{\text{B}} = 1.186 \pm 0.005$.

HD 216494 is actually a stable hierarchical triple system: a pair, composed by the spectroscopic binary described in the previous paragraph, plus a single third component discovered during a speckle interferometric survey carried out at the 4-m Kitt Peak telescope by McAlister et al. (1987). Subsequent speckle observations are due to McAlister, Hartkopf & Franz (1990) and Tokovinin (1993) who derived a period of 19.25 yr. Later, Mason (1997), by combining literature and his own speckle observations, obtained with the method of lunar occultations, computed a new set of parameters for the outer orbit: $P = 18.13 \pm 0.26$ yr, $i = 64.5^\circ \pm 1.6^\circ$, $a = 0.0783 \pm 0.0013$ arcsec and $e = 0.063 \pm 0.016$. According to *Hipparcos* satellite (ESA 1997), $d = 202 \pm 34$ pc, so we estimate that the semimajor axis of the orbit of the wide pair is ≈ 16 au.

Hubrig & Mathys (1995) observed spectral evidence of the third component, in particular they identified a broad feature above the

[★]Based on data obtained from the ESO Science Archive Facility under request number GCATANZARO43200 and GCATANZARO43204.

[†]Partially based on observations made with the INAF – Catania Astrophysical Observatory telescope.

[‡]E-mail: gca@oact.inaf.it

[§]Guest User, Canadian Astronomy Data Centre, which is operated by the Dominion Astrophysical Observatory for the National Research Council of Canada's Herzberg Institute of Astrophysics.

two sharp Mg II $\lambda 4481$ lines of both components. These authors suggested that the spectral type of HD 216494 C could be similar to or slightly earlier than that of the primary.

The presence of the third companion in the spectra of the SB2 system, from now on SB3, has been definitively confirmed by Catanzaro & Leto (2004). They identified the signature of the H β profile of HD 216494 C in their six spectra obtained at INAF – Catania Astrophysical Observatory. No further details about its atmospheric abundances could be provided from those spectra.

The aim of this study is to determine fundamental atmospheric parameters and chemical abundances for the three components with particular attention to the real nature of HD 216494 C.

3 OBSERVATIONS AND DATA REDUCTION

Atmospheric parameters and chemical abundances for HD 216494 components have been derived from spectra obtained at the 0.9-m telescope of the Catania Astrophysical Observatory (OAC) in the 4810–5370 Å spectral region with the fibre-linked REOSC echelle spectrograph. The resolving power deduced from the lines of the Th–Ar lamp is $\approx 20\,000$. The achieved signal-to-noise ratio (S/N) was ≈ 100 (Catanzaro & Leto 2004).

Furthermore, spectra of the HD 216494 system have been downloaded from the archives of two different telescopes.

(i) Three spectra have been obtained on 1995 September 8–10 at the 3.6-m telescope of the Canada–France–Hawaii Telescope (CFHT) equipped with the $f/4$ coudé (*Gecko*) spectrograph. The resolution as deduced from the full width at half-maximum (FWHM) of Th–Ar comparison lamp lines is about 100 000. The achieved S/N was larger than 300.

(ii) Six spectra have been acquired on 1999 December 17 with the Very Large Telescope ultraviolet (UV) visual echelle spectrograph (UVES@UT2, program ID 60.A-9022). Three exposures in the blue arm have been recorded with the order separation filter CuSO₄ and grating CD#2 covering the spectral range between 3280 and 4520 Å and three in the red arm with the SHP700 filter and CD#3 grating covering the region 4600–6680 Å. Combining these images, we obtained a final spectrum with S/N up to 500. From the lines of the Th–Ar calibration lamp, we measured the final resolving power that is $\approx 60\,000$ in the blue arm and $\approx 70\,000$ in the red arm.

The stellar spectra, calibrated in wavelength and with the continuum normalized to a unity level, were obtained using standard data reduction procedures for spectroscopic observations within the NOAO/IRAF package.

4 STELLAR PARAMETERS

Among the various methods commonly used to determine effective temperature (T_{eff}) and gravity ($\log g$) of a star, the comparison between the observed and theoretical profile of a Balmer line is particularly suitable for our purpose. In the case of this SB3 system, the observed H β profile is actually given by the superposition of lines Doppler shifted by the orbital motion of the three components and weighted by relative luminosities.

In this study, we used the H β profile obtained at the OAC at the orbital phase $\phi = 0.20$, when the separation between components A and B was maximum (Catanzaro & Leto 2004). This procedure took into account simultaneously the spectra of the three components. A grid of atmospheric models has been calculated with ATLAS9 (Kurucz 1993), for $\xi = 0 \text{ km s}^{-1}$ and ODF = [0.0] (solar metal opacity), and the synthetic H β with SYNTH3 (Kurucz & Avrett 1981). The grid

extends over the intervals $9000 \leq T_{\text{eff}} \leq 15\,000 \text{ K}$ (step of 100 K) and $3.5 \leq \log g \leq 4.5$ (step of 0.1 dex).

The synthetic spectrum normalized to the unity level has been derived following the formula:

$$F_{\text{Tot}} = \frac{F_A + F_B + F_C}{I_A + I_B + I_C}, \quad (1)$$

where $F_{A,B,C}$ and $I_{A,B,C}$ are, respectively, computed fluxes and continua of each component.

To reduce the number of parameters, first we have determined the rotational velocities of HD 216494 A, B and C by matching metal lines with synthetic profiles in our highest resolution (CFHT) spectra. The best fit occurs for a rotational velocity of 1 km s^{-1} for A and B components, while for the C component we found $v_e \sin i = 130 \text{ km s}^{-1}$.

Leone & Manfè (1996) and later Catanzaro, Leone & Dall (2004) showed the importance of a correct helium abundance assumption in determining the effective temperature and gravity of stars. Particularly, helium can be largely underabundant in HgMn stars as shown by several analyses reported in the literature (i.e. Adelman, Ryabchikova & Davydova 1998; Catanzaro, Leone & Leto 2003). In a recent work, Dworetzky (2004) studied the helium abundances in a sample of 25 HgMn stars. He found that helium deficiency was temperature dependent, with deficiencies tending to be more pronounced at higher temperatures. T_{eff} and $\log g$ values, obtained assuming solar abundance of helium, have been used to start an iterative procedure necessary to derive the stellar parameters consistent with the helium abundance.

To fix the helium content in all components, we considered the spectral region centred around He I $\lambda 4471 \text{ Å}$ observed with UVES. The synthetic spectrum, computed using SYNTH3 and ATLAS9 models computed with solar ODF, shows that helium is strongly underabundant in the atmospheres of A and B components while it is almost solar in the C component. Our adopted values are $\log(N_{\text{He}}/N_{\text{tot}}) = -1.70, -1.82$ and -1.10 , for A, B and C components, respectively.

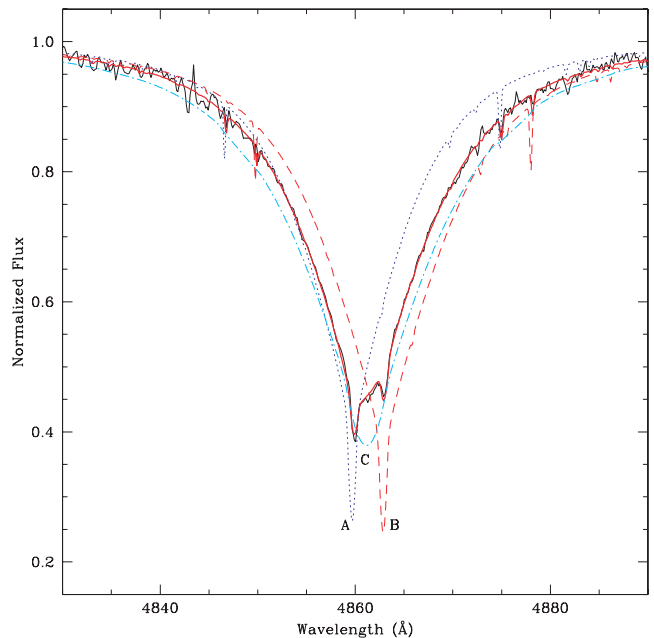


Figure 1. Comparison between the observed and computed H β line profiles. Synthetic profile is the combination of HD 216494 A (dotted line), HD 216494 B (dashed line) and HD 216494 C (dot-dashed line).

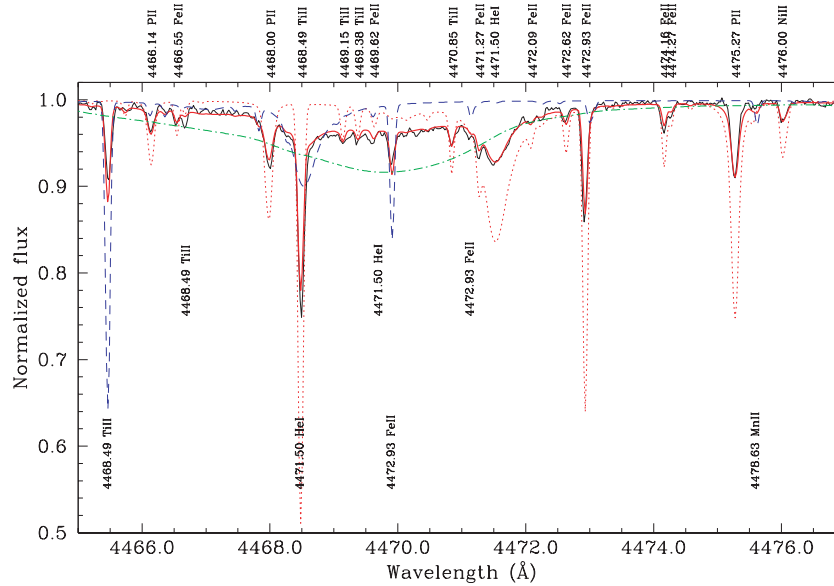


Figure 2. Composed synthetic spectrum (solid line) of the region centred around $\lambda 4471 \text{ \AA}$ compared with the observations. Labels above the continuum refer to primary, those below the spectrum to the secondary and those in the middle refer to the tertiary.

Table 1. Atmospheric parameters adopted in our study for the three components of HD 216494.

HD 216494	T_{eff} (K)	$\log g$	$v \sin i$ (km s^{-1})
A	12 000	3.7	1.0 ± 0.5
B	11 500	3.9	1.0 ± 0.5
C	11 500	4.1	130 ± 20

ATLAS9 code computes the continuum opacity according to the assumed helium abundance, however the influence of helium on metal opacity has been evaluated for the solar helium abundance and a complete helium absence¹ only. To check the consistence of previously determined stellar parameters, we repeated the iterative procedure on the basis of models, for A and B components, computed with an *ODF* evaluated for null helium abundance. This new calculation gives the T_{eff} and $\log g$ reported in Table 1. The final synthetic $H\beta$ computed with these values has been compared in Fig. 1 with the observation. The previous helium abundances are confirmed also for the new atmosphere models (see Fig. 2 for details). Errors in T_{eff} and $\log g$ have been estimated as the variation in the parameters which increases the χ^2 by a unit. We found $\delta T \approx 150 \text{ K}$ and $\delta \log g \approx 0.1 \text{ dex}$ values consistent with the step adopted in our grid of models.

In the next section, we will show that the effective temperatures and gravities determined for the A and B components are compatible with the ionization balance between neutral and once ionized iron.

5 ABUNDANCE ANALYSIS

The approach used in this paper to determine stellar abundances was to compute the synthetic spectrum that best reproduce the observed

one with UVES. This is because of the intrinsic difficulty in determining the true equivalent widths of metal lines that are strongly reduced by the dilution effect caused by the superposition of the fluxes of three components.

We divided all spectral range covered by our data in 118 subintervals 25-\AA wide each. For each interval, we derived the abundances by a χ^2 minimization of the difference between the observed and synthetic total spectrum. Line lists and atomic parameters used in our modelling are from Kurucz & Bell (1995) as updated by Castelli & Hubrig (2004). During our analysis, we found in the NIST data base improved $\log gf$ for a few transitions, namely P II $\lambda\lambda$ 4466.14, 4475.27 \AA and a blend of Mg II composed of three lines, $\lambda\lambda$ 6346.754, 6346.762 and 6346.964 \AA .

In Table 2, we report the abundances derived in our analysis expressed in the usual logarithmic form relative to the total number of atoms N_{tot} . To easily compare the chemical pattern of HD 216494, we report in the last column the solar abundances taken from Asplund, Grevesse & Sauval (2005). To make these values directly comparable with our abundances, we changed the scale $\log(N_{\text{elem}})$ relative to $\log(N_{\text{H}}) = 12$ to the scale relative to $\log(N_{\text{tot}})$. Error reported in Table 2 for a given element is the standard deviation on the average computed among the various abundances determined in each subinterval. When a given element appeared in one or two subintervals only, the error on its abundance evaluated varying temperature and gravity in the ranges $[T_{\text{eff}} \pm \delta T_{\text{eff}}]$ and $[\log g \pm \delta \log g]$ is typically 0.1 dex.

As a check for the goodness of our T_{eff} and $\log g$ determined for the A and B components, we could consider the consistency of the abundances derived from spectral lines of iron in the first two stages of ionization: -3.75 ± 0.12 and -3.90 ± 0.13 for Fe I and Fe II in the primary component and -4.65 ± 0.10 and -4.70 ± 0.16 for Fe I and Fe II in the secondary component. The adopted iron abundances reported in Table 2 are the averages between these two values.

In the following sections, we discuss the abundances derived for each component. For each star, we comment on the results for light elements (from helium to calcium), iron group elements (from scandium to nickel) and present heavier elements from gallium to mercury.

¹ <http://kurucz.harvard.edu/opacities.html>

Table 2. Abundances derived for HD 216494 A, B and C expressed in terms of $\log N(\text{el})/N_{\text{tot}}$ compared with the solar values (Asplund et al. 2005). For the B component, missing abundances are smaller than solar values. Due to the high rotational velocity of the C component, only for a few elements was it possible to obtain an abundance value.

Elements	A	B	C	Sun
He	-1.70	-1.82	-1.10	-1.10
C	≤ -4.90	-3.90		-3.64
N	≤ -4.50	≤ -4.50		-4.25
O	-3.60	-3.55	-3.20	-3.37
Ne	-4.20			-4.19
Na	-5.30	-5.30	-5.70	-5.86
Mg	-4.74 ± 0.20	-4.85 ± 0.15	-4.36	-4.50
Al	≤ -7.20	-5.90		-5.66
Si	-4.26 ± 0.19	-4.90	-4.20	-4.52
P	-4.39			-6.67
S	-5.41 ± 0.35	-4.75		-4.89
Ca	-5.64	-6.00	-5.90	-5.72
Sc	-9.10	-9.30		-8.98
Ti	-6.35 ± 0.25	-7.20 ± 0.20	-7.00	-7.13
V	≤ -8.50	≤ -8.24		-8.03
Cr	-6.48 ± 0.14	-6.70		-6.39
Mn	-5.15 ± 0.17			-6.64
Fe	-3.82 ± 0.18	-4.67 ± 0.19	-4.50	-4.58
Co	≤ -8.10			-7.11
Ni	-6.79			-5.80
Ga	-4.96 ± 0.16			-9.15
Sr	-9.70	-8.70		-9.11
Zr	-8.25			-9.44
Xe	-5.00			-9.76
Pr	-9.40	-8.50		-11.32
Nd	-8.80	-9.00		-10.58
Au	-7.20			-11.02
Hg	-6.40			-10.90

5.1 HD 216494 A

Light elements. Principal anomalies derived for the primary component are the underabundances of helium and aluminium, for which we obtained $\log(N_{\text{el}}/N_{\text{tot}}) = -1.70$ and -7.20 , respectively, and the strong abundance of phosphorus, ≈ 2.2 dex over the solar value. Actually for aluminium, we could measure only an upper limit value.

For the other light elements, we did not obtain abundances significantly different from the solar. In particular, we could measure the sodium abundance from the doublet at 5890 Å, well separated from the interstellar medium lines because of the large wavelength shift due to the orbital motion. Those lines have been used even in the other two components.

Iron group elements. Strong overabundances have been detected for titanium (≈ 0.7 dex over the solar value), manganese (≈ 1.5 dex) and iron (≈ 0.7 dex). For two elements, we obtained abundances under the solar values, namely, cobalt, for which we could assess only an upper limit of -8.10 and nickel, with an underabundance of ≈ 1 dex.

Lines of the other elements detected in our spectra (i.e. scandium, vanadium and chromium) are compatible with almost solar abundances.

Heavy elements. With the exception of strontium, for which an underabundance of ≈ 1 dex has been derived, overabundances of gallium (≈ 4.2 dex), zirconium (≈ 1.2 dex), xenon (≈ 4.7 dex), praseodymium (≈ 2 dex), neodymium (≈ 1.7 dex), gold (≈ 3.8 dex)

and mercury (≈ 4.5 dex) were observed in the atmosphere of HD 216494 A.

In the following section, we discuss separately the isotopic structure of manganese, gallium and mercury.

5.1.1 Manganese, gallium and mercury

Often, heavy elements shows spectral lines split because of the various stable isotopes of that given atom or by hyperfine structure. For example, atoms like manganese, gallium, platinum and mercury are well known to show this effect (Smith 1997; Hubrig, Castelli & Mathys 1999; Catanzaro et al. 2003; Castelli & Hubrig 2004).

Abundances of manganese in a sample of HgMn stars have been studied by Jomaron, Dworetzky & Allen (1999). These authors demonstrated that hyperfine structure is responsible for the line strength anomalies seen in lines such as Mn II $\lambda 4326$ and $\lambda 4206$ Å. In our study, we selected the four Mn II lines for which their hyperfine structure has been measured in the laboratory by Holt, Scholl & Rosner (1999). The results of our calculations are shown in Fig. 3; in each plot, we report the abundance derived from the synthesis of each single line. The average value is -5.15 ± 0.17 .

For gallium, we selected the four Ga II lines in the 4250–4262 Å region and the Ga II $\lambda 6334$ Å which is the strongest line in the red part of our UVES spectrum. For the spectral synthesis of the four blue lines, we used both atomic parameters from Dworetzky, Jomaron & Smith (1998) (solid lines in Fig. 4) and Ryabchikova & Smirnov (1994) (dashed lines in Fig. 4). For the red line showed in Fig. 5, we used only the Ryabchikova & Smirnov (1994) atomic parameters. In our synthesis, we took into account the Cr II $\lambda 4261.847$, 4261.913 Å lines that blend the Ga II $\lambda 4262$ Å in its blue wing and the Ne I $\lambda 6334.428$ that blend the Ga II $\lambda 6334$ in its red wing.

Blue lines are generally better reproduced adopting Dworetzky et al. (1998) hfs model, with the exception of Ga II $\lambda 4255$ Å for which parameters by Ryabchikova & Smirnov (1994) give the best result. The red wing of the Ga II $\lambda 4262$ is not well fitted probably

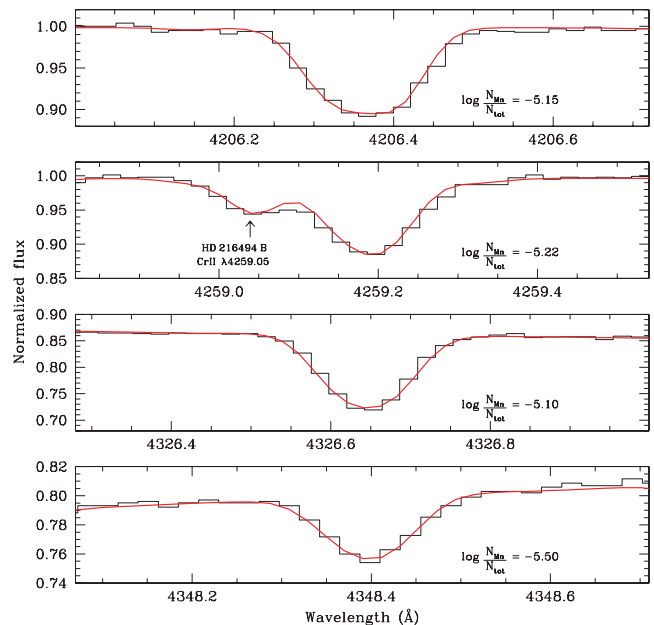


Figure 3. Comparison between observed (histogram) and computed (solid) profiles for the four Mn II lines discussed in the text. In each window, we reported the relative abundance.

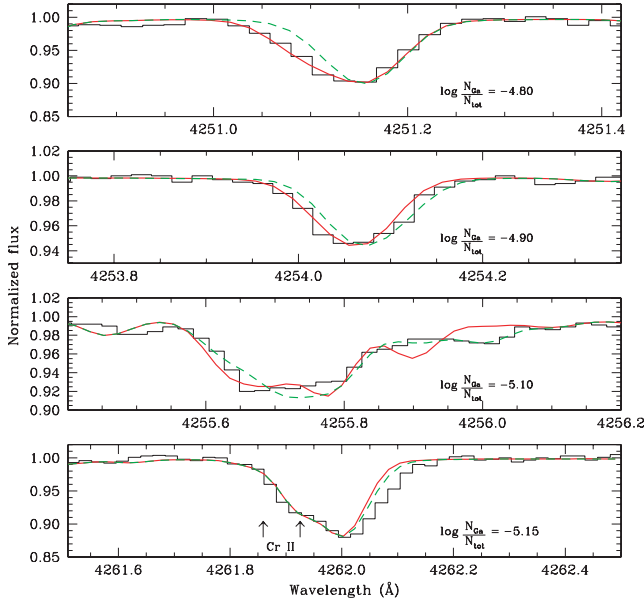


Figure 4. Comparison between observed (histogram) and computed (solid) profiles for the four blue Ga II lines discussed in the text. In each window, we reported the relative abundance used for the synthetic profiles, the one calculated using Dworetzky et al. (1998) hfs model (solid line) and the one computed using Ryabchikova & Smirnov (1994) (dashed line) atomic parameters.

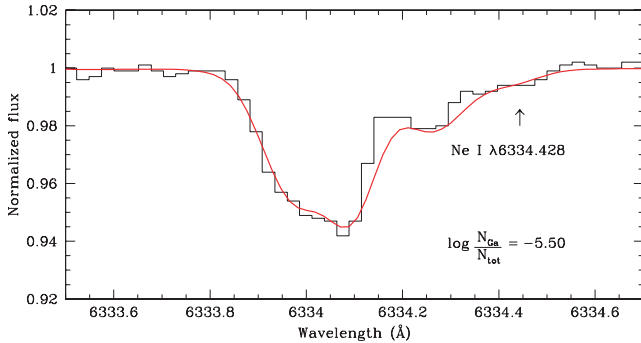


Figure 5. Comparison between observed (histogram) and computed profiles (solid) for the red Ga II line λ 6334 Å.

for some unidentified blend at λ 4262.090, as already observed in many other HgMn stars by Dworetzky et al. (1998).

The gallium abundance derived from the red line is significantly lower than those computed from the blue lines. Since there are no direct measurement of the $\log gf$ of this line (Dworetzky et al. 1998), we prefer to adopt as gallium abundance for HD 216494 A the mean value obtained from the blue lines only, that is -4.96 ± 0.16 .

For mercury, we have $R \approx 100\,000$ spectra, as downloaded from the CFHT archive, covering the region around the Hg II λ 3984 Å. In general, the profile of this line in HgMn stars can be a blend of seven stable isotopes of mercury ($A = 196, 198, 199, 200, 201, 202, 204$) of which those with odd isotope numbers are further split into hyperfine components (Dworetzky, Ross & Aller 1970).

Woolf & Lambert (1999) noted that HD 216494 A shows an isotopic mixture of mercury very close to the terrestrial one with an abundance of ≈ -6.80 dex. A very similar result has been obtained by Hubrig et al. (1999), they fitted their observed profile with an

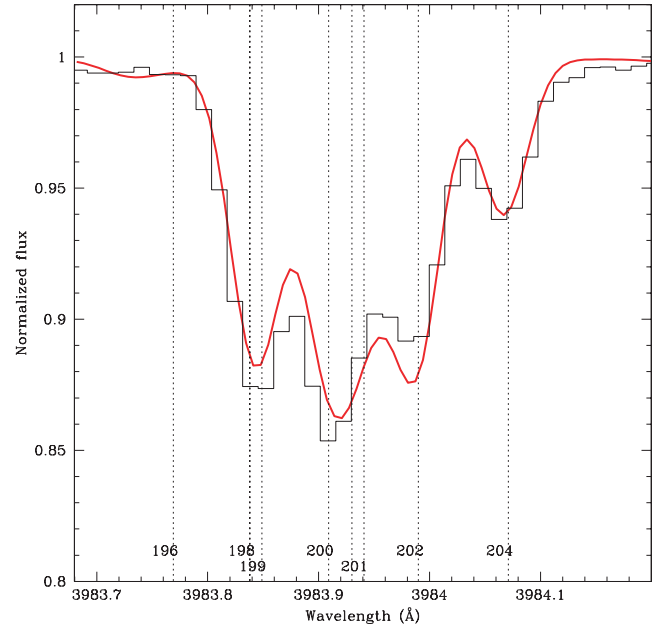


Figure 6. The observed (histogram) complex line profile of the Hg II λ 3984 Å line is matched (solid line) with a synthetic line computed with $\log N_{\text{Hg}}/N_{\text{tot}} = -6.40$ and terrestrial mercury isotopic mixture as previously proposed by Woolf & Lambert (1999).

ad hoc isotopic mixture that is compatible with an abundance of $\log N_{\text{Hg}}/N_{\text{tot}} = -6.95$.

In this study, to determine the Hg abundance we proceeded to modify its value by trial and error, until achieving a good agreement between the observed and computed total equivalent width of this spectral line. For our calculation, we adopted $\log gf = -1.520$ (Castelli & Hubrig 2004) for the all transition responsible for the Hg II line, while wavelengths for each isotopic transition and terrestrial isotopic mixture have been taken from Smith (1997). The synthetic line shown in Fig. 6 has been computed for $\log N_{\text{Hg}}/N_{\text{tot}} = -6.40$.

The discrepancy between our Hg abundance and previous values is due to the fact that latter authors did not consider the presence of the third component that strongly affects the continuum.

5.2 HD 216494 B

Light elements. The only significantly anomaly found in this group of elements is that concerning helium underabundance, that is ≈ 0.7 dex smaller than the Sun. Other light elements are almost normal.

Iron group elements. No significative anomalies in the abundances of the iron peak elements have been determined for HD 216494 B.

Heavy elements. Only spectral lines of three heavy elements have been observed in this component and all of them appear to be overabundant. In particular, we found strontium ≈ 0.4 dex, praseodymium ≈ 2.8 dex and neodymium ≈ 1.6 . Contrarily to the primary, no lines of Hg have been detected.

5.3 HD 216494 C

Because of its high rotational velocity, it was really difficult to identify spectral lines belonging to the C component. As an example, in Fig. 7 we show the spectral region from λ 5035 Å to λ 5060 Å,

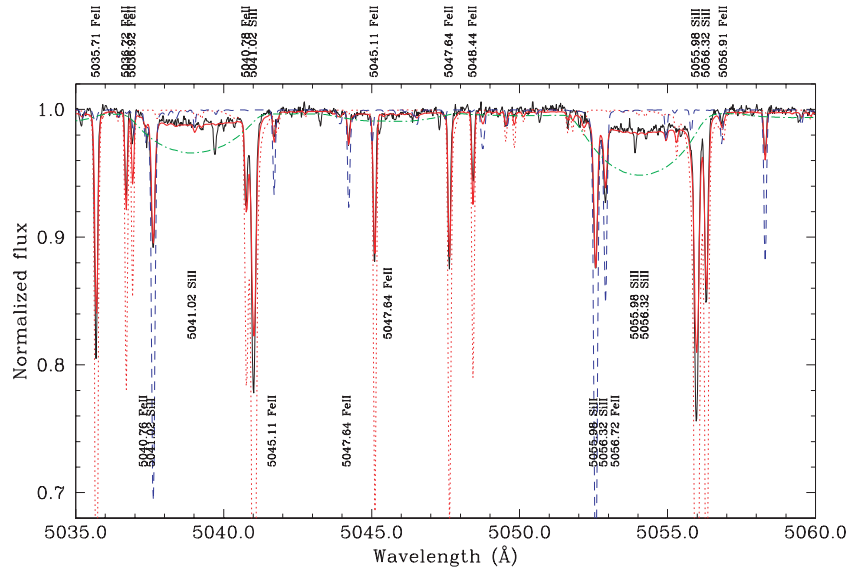


Figure 7. Composed synthetic spectrum (solid line) of the region centred around $\lambda 5047$ Å compared with the observations. Symbols as in Fig. 2

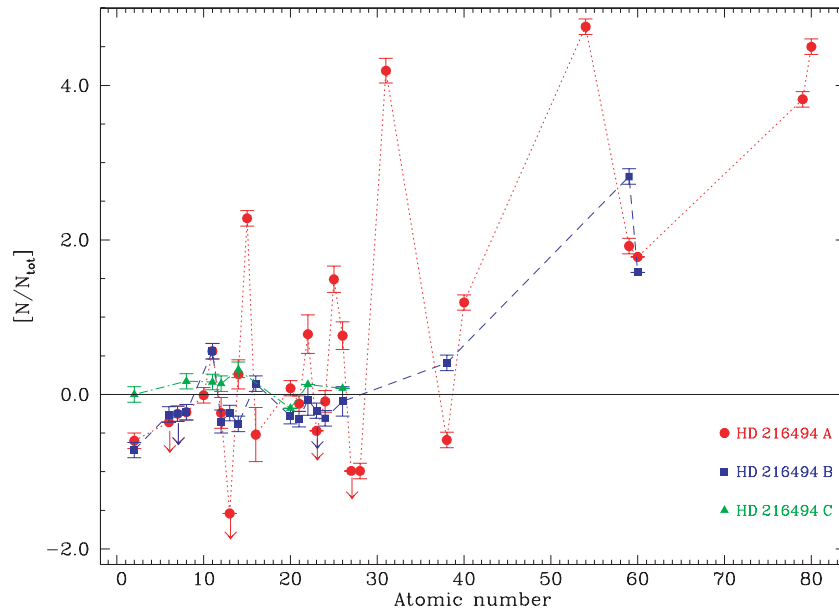


Figure 8. Abundance patterns for the three components of HD 216494. Circles connected by dotted line represent the pattern of the primary, boxes connected by dashed line are relative to the secondary and the triangles connected by dot-dashed line are the pattern of the tertiary. The solid line represents the solar abundances. Elements for which we found only an upper limit are represented by an arrow.

with overimposed the synthetic spectrum calculated in this study, which are clearly visible the contribution of HD 216494 C to the total spectrum.

As a result, we identified features belonging to six light elements, namely, He, O, Na, Mg, Si and Ca and to two elements of the iron group, i.e. titanium and iron (see Fig. 7 as an example). For all these elements, we derived almost solar abundances.

6 CONCLUSIONS

In this paper, we determined the abundance pattern of the three components of the SB3 system HD 216494 (see Fig. 8). The most puzzling star of the system is certainly the primary: it shows

the typical features of the HgMn subclass, i.e. extreme overabundance of phosphorous, iron, manganese, gallium, neodymium, praseodymium, gold and mercury and a helium abundance lower than solar. On the other hand, it shows also an underabundance of strontium that in HgMn is typically higher than the Sun value.

The only anomalies shown by the B component are the underabundance of helium and the overabundance of praseodymium and neodymium, even if the abundances of these two elements have been derived, respectively, from two lines (Pr III $\lambda\lambda 5284.68, 5299.97$ Å) and one line (Nd III $\lambda 5294.11$ Å) only. The other elements have a standard abundance or, in some case, slightly lower. Mathys & Hubrig (1995) measured the effective magnetic fields of this component obtaining $B_{\text{eff}} = -375 \pm 142$ and -270 ± 86 G in two

nights. As a consequence, we conclude that HD 216494 B may be a magnetic chemically peculiar star.

HD 216494 C appeared to be the only normal star of the system. Because of its high rotational velocity ($v \sin i = 130 \text{ km s}^{-1}$), it was difficult to identify its spectral lines in the observed spectra. Weak lines are much broadened by the rotation and are at the noise level with the continuum, and only a few strong lines belonging to different elements could be clearly detected. They are all compatible with solar abundances.

As a general conclusion, the SB3 system HD 216494 is composed of three stars with similar effective temperature but with very different abundance patterns. If, as expected, the three components are coeval and formed in a region homogeneous in the chemical composition, the observed chemical anomalies of upper main-sequence stars are related to the stellar properties (i.e. rotational velocity) and they are not only a characteristic of the progenitor cloud.

ACKNOWLEDGMENTS

This research has made use of the SIMBAD database, operated at CDS, Strasbourg, France.

Thanks are due to the referee, Mike Dworetzky, for his critical and helpful revision of the original manuscript.

REFERENCES

- Adelman S. J., Ryabchikova T. A., Davydova E. S., 1998, *MNRAS*, 297, 1
 Asplund M., Grevesse N., Sauval A. J., 2005, in Barnes T. G., III, Bash F. N., eds, ASP Conf. Ser. Vol. 336, *Cosmic Abundances as Records of Stellar Evolution and Nucleosynthesis*. Astron. Soc. Pac., San Francisco, p. 25
 Castelli F., Hubrig S., 2004, *A&A*, 425, 263
 Catanzaro G., Leto P., 2004, *A&A*, 416, 661
 Catanzaro G., Leone F., Leto P., 2003, *A&A*, 407, 669
 Catanzaro G., Leone F., Dall T. H., 2004, *A&A*, 425, 641
 Dworetzky M. M., 2004, in Zverko J., Ziznovsky J., Adelman S. J., Weiss W. W., eds, Proc. IAU Symp. 224, *The A Star Puzzle*. Cambridge Univ. Press, Cambridge, p. 727
 Dworetzky M. M., Ross J. E., Aller L. H., 1970, *BAAS*, 2, 311
 Dworetzky M. M., Jomaron C. M., Smith C. A., 1998, *A&A*, 333, 665
 ESA, 1997, SP-1200, *The Hipparcos Catalogue*
 Holt R. A., Scholl T. J., Rosner S. D., 1999, *MNRAS*, 306, 107
 Hubrig S., Mathys G., 1995, in Sauval A. J., Blomme R., Grevesse N., eds, ASP Conf. Ser. Vol. 81, *Laboratory and Astronomical High Resolution Spectra*. Astron. Soc. Pac., San Francisco, p. 555
 Hubrig S., Castelli F., Mathys G., 1999, *A&A*, 341, 190
 Jomaron C. M., Dworetzky M. M., Allen C. S., 1999, *MNRAS*, 303, 555
 Kurucz R. L., 1993, in Dworetzky M. M., Castelli F., Faraggiana R., eds, ASP Conf. Ser. Vol. 44, *IAU Colloquium 138, Peculiar Versus Normal Phenomena in A-Type and Related Stars*. Astron. Soc. Pac., San Francisco, p. 87
 Kurucz R. L., Avrett E. H., 1981, *SAO Special Rep.*, 391
 Kurucz R. L., Bell B., 1995, Kurucz CD-ROM No. 23. Smithsonian Astrophysical Observatory, Cambridge, MA
 Leone F., Manfrè M., 1996, *A&A*, 315, 526
 Mason B. D., 1997, *AJ*, 114, 808
 Mathys G., Hubrig S., 1995, *A&A*, 293, 810
 McAlister H. W., Hartkopf W. I., Hutter D. J., Franz O. G., 1987, *AJ*, 93, 688
 McAlister H. W., Hartkopf W. I., Franz O. G., 1990, *AJ*, 99, 965
 Michaud G., 1970, *ApJ*, 160, 641
 Ryabchikova T. A., Smirnov Yu. M., 1994, *Astron. Rep.*, 38, 1
 Smith K. C., 1997, *A&A*, 319, 928
 Tokovinin A. A., 1993, *Sov. Astron. Lett.*, 19, 383
 Wolff R. J., 1974, *PASP*, 86, 173
 Woolf V. M., Lambert L., 1999, *ApJ*, 521, 414
 Wolff S. C., Wolff R. J., 1974, *ApJ*, 194, 65

This paper has been typeset from a $\text{\TeX}/\text{\LaTeX}$ file prepared by the author.